



# Impact of the $\Delta$ Phe configuration on the Boc-Gly- $\Delta$ Phe-NHMe conformation: experiment and theory

Aneta Buczek<sup>1</sup> · Dawid Siodłak<sup>1</sup> · Maciej Bujak<sup>1</sup> · Maciej Makowski<sup>1</sup> · Teobald Kupka<sup>1</sup> · Małgorzata A. Broda<sup>1</sup>

Received: 4 June 2019 / Accepted: 25 June 2019 / Published online: 18 July 2019  
© The Author(s) 2019

## Abstract

Conformational propensities of *N*-*t*-butoxycarbonyl-glycine-(*E/Z*)-dehydrophenylalanine *N*'-methylamides (Boc-Gly-(*E/Z*)- $\Delta$ Phe-NHMe) in chloroform were investigated by NMR and IR techniques. The low-temperature crystal structure of the *E* isomer was determined by single crystal X-ray diffraction and the experimental data were elaborated by theoretical calculations using DFT (B3LYP, M06-2X) and MP2 approaches. The  $\beta$ -turn tendencies for both isomers were determined in the gas phase and in the presence of solvent. The obtained results reveal that the configuration of  $\Delta$ Phe residue significantly affects the conformations of the studied dehydropeptides. The tendency to adopt  $\beta$ -turn conformations is significantly lower for the *E* isomer (Boc-Gly-(*E*)- $\Delta$ Phe-NHMe), both in gas phase and in chloroform solution.

**Keywords** <sup>1</sup>H NMR · <sup>13</sup>C NMR · IR spectroscopy · X-ray crystal structure analysis · Peptide conformational analysis ·  $\beta$ -turn tendency · DFT-GIAO calculations · Dehydrophenylalanine · *Z* isomer · *E* isomer

## Introduction

Biological activity of numerous small size molecules is directly related to their conformational properties. It is possible to control pharmaco-kinetic properties of naturally occurring peptides by introduction of nonstandard amino acid residues into their backbone chain which could produce derivatives showing more desired pharmacological properties, for example, resistance to enzymatic degradation, receptor selectivity, enhanced potency, or bioavailability [1–5]. For example, it is possible to introduce a dehydroamino acid residue and forcing a specific conformation of the chain fragment [6].

$\alpha,\beta$ -Dehydroamino acids are non-coded amino acids [7, 8] in which the  $C^\alpha = C^\beta$  bond freezes the  $\chi^1$  torsion angle and sets the  $\beta$ -substituents in *Z* or *E* position.

Both isomers of the dehydroresidues occur in nature and they often exhibit different biological properties [7, 9].  $\alpha,\beta$ -Dehydropeptides are more stable and resistant toward proteolytic degradation and thus could be used to design synthetic analogs of biologically active peptides [10–12]. According to the literature on  $\alpha,\beta$ -dehydropeptides, the (*Z*)-dehydrophenylalanine [13–15] is the most often studied residues. It is known that (*Z*)- $\Delta$ Phe residue stabilizes  $\beta$ -turns in short peptides and  $3_{10}$  helix in longer ones [13, 16]. The conformational profile of the isomer *E* is much less recognized. According to literature data, (*E*)- $\Delta$ Phe adopts in its crystal structure the  $\beta$  ( $\phi, \psi \sim -42^\circ, 124^\circ$ ) conformation or the helical  $\alpha_L$  ( $\phi, \psi \sim 51^\circ, 49^\circ$ ) one [17–20]. In non-polar solvents, the extended conformer  $C_5$  ( $\phi, \psi \sim -179^\circ, 162^\circ$ ) can be also found [21]. Spectroscopic and theoretical investigations of dehydropeptides analogs with *E* or *Z* isomers of dehydroamino acid residues in peptide chain suggest their different conformational preference in solution [22–26] has different conformational preferences in solution.

Our DFT study on Ac-Gly-(*E/Z*)- $\Delta$ Phe-NHMe [26] pointed out that (*E*)- $\Delta$ Phe has strong tendency to adopt the extended conformation while the *Z* isomer of Ac-Gly- $\Delta$ Phe-NHMe has the disposition to occur in the gas

**Electronic supplementary material** The online version of this article (<https://doi.org/10.1007/s11224-019-01387-w>) contains supplementary material, which is available to authorized users.

✉ Małgorzata A. Broda  
Malgorzata.Broda@uni.opole.pl

<sup>1</sup> Faculty of Chemistry, Opole University, Oleska 48,  
45-052 Opole, Poland

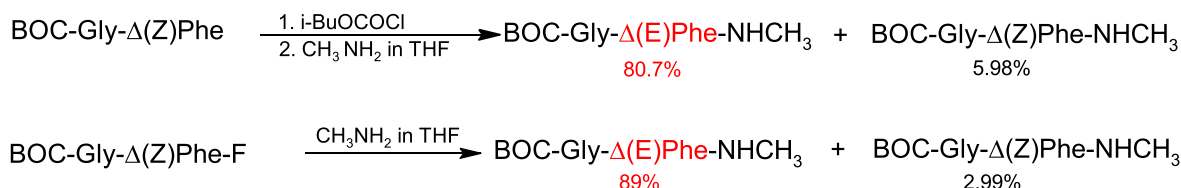
phase as type II and in solvents as type I  $\beta$ -turn conformation. However, the dihedral angles  $\phi_1$ ,  $\psi_1$ , and  $\phi_2$ ,  $\psi_2$  are uncommon in standard amino acids.

The aim of the current study is to support the above theoretical results by experimental data. We were interested in determination of the impact of dehydrophenylalanine configuration on the formation of  $\beta$ -turn by the peptide backbone. Thus, we report on the single crystal X-ray study of *E* isomer of N- and C-protected dipeptide Boc-Gly- $\Delta$ Phe-NHMe. In

addition, we conducted spectroscopic (FTIR and NMR) conformational research for both *E* and *Z* isomers and detailed theoretical analysis.

## Experimental procedures

### Synthesis of peptides



### Boc-Gly- $\Delta$ Phe-NHCH<sub>3</sub>

*Z* and *E* isomers of Boc-Gly- $\Delta$ Phe-NHMe, abbreviated as compounds **(1)** and **(2)**, were derived from Boc-Gly-(*Z*)- $\Delta$ Phe, synthesized using a previously reported methodology [27, 28]. In particular, *solution 1* was obtained following a simple procedure using THF (2.5 mL) cooled to  $-18$  °C and next saturated with methylamine (30 min). Subsequently, the temperature of Boc-Gly-(*Z*)- $\Delta$ Phe (solution of 0.161 g, 0.5 mmol) and TEA (0.07 mL, 0.5 mmol in 2.5 mL of THF) was decreased to  $-15$  °C and subsequently, 0.065 mL, (0.5 mmol) of isobutyl chloroformate was added and next (after about 90 s) *solution 1* was poured in. The obtained liquid mixture was saturated with methylamine for 30 min and mixed (22 h) at room temperature. The excess of THF was evaporated and the oily residue dissolved in 2.5 mL of ethyl acetate. As result, a mixture of (*Z*) and (*E*) isomers was obtained. The two isomers were separated with the help of column chromatography filled with silica gel H60 (Merck). As eluent methanol in ethyl acetate was selected (from 0.05 to 0.45% of methanol). The individual components were obtained in a crystalline form from a solution CHCl<sub>3</sub> - diethyl ether (1:20, v/v)/hexane. The following yield of products was obtained: isomer *E* 0.135 g (80.7%); mp 180–182 °C, isomer *Z* 0.01 g (5.98%); mp 193–195 °C.

In parallel, a second procedure was used 0.094 mL of diisopropylethylamine (DiPEA, 0.55 mM) in 1.25 mL of THF cooled to  $-20$  °C, saturated 30 min with methylamine. In the next step Boc-Gly-(*Z*)- $\Delta$ Phe-F solution (0.177 g, 0.55 mM as fluorine source) in 1.25 mL THF was added to *solution 1*, saturated with methylamine for 20 min and next mixed 22 h at 298 K. The remaining synthesis stages were identical as for the first procedure. The total yield of this

synthesis was 0.149 g (89%) for isomer *E* (mp. 180–182.5 °C) and 0.005 g (2.99%) for isomer *Z* (mp. 194–196 °C). The results of elemental analysis are as follows: calcd. (%) for C<sub>17</sub>H<sub>23</sub>N<sub>3</sub>O<sub>4</sub> (334.395), C—61.25%, H—6.95%, N—12.60%; found (*Z*): C—61.17%, H—6.89%, N—12.66%; (*E*): C—61.15%, H—6.83%, N—12.67%.

### X-ray crystal structure analysis

The low-temperature (85 K) intensity data for Boc-Gly-(*E*)- $\Delta$ Phe-NHMe were measured on an Xcalibur diffractometer, using the graphite monochromated MoK $\alpha$  ( $\lambda = 0.71073$  Å) radiation, and a cooler made by Oxford Cryosystems. The *CrysAlis CCD* and *CrysAlis Pro* programs enable both data collection and cell refinement, as well as entire processing of data reduction [29]. The crystal structure was obtained from direct methods and additionally refined on  $F^2$ , applying a full-matrix least-squares method with the help of SHELX program [30]. The positions of all non-H atoms were subsequently refined using anisotropic displacement parameters. On the contrary, the hydrogen atoms were located using Fourier difference maps. Hydrogen atoms directly attached to nitrogen atoms were refined using geometrical restraints (SADI command of SHELXL) [30]. The riding model, incorporating idealized structural parameters, including bond lengths and angles, was applied to the remaining hydrogen atoms. The isotropic displacement parameters of hydrogen atoms were taken with coefficients 1.5 and 1.2 times higher than the corresponding ones methyl carbon and the remaining carbon/nitrogen atoms, respectively. Structural drawings were obtained with *Mercury* program [31].

### Crystal data for Boc-Gly-(*E*)- $\Delta$ Phe-NHMe

$C_{17}H_{23}N_3O_4$ ,  $M = 333.38$ , crystal size  $0.48 \times 0.48 \times 0.25$  mm, monoclinic, space group  $P2_1/c$ ,  $a = 17.0537$  (6),  $b = 5.9680$  (2),  $c = 17.6177$  (5) Å,  $\beta = 103.647$  (3)°,  $V = 1742.45$  (10) Å<sup>3</sup>,  $\rho_{\text{calcd}} = 1.271$  g/cm<sup>3</sup>,  $Z = 4$ ,  $\mu = 0.092$  mm<sup>-1</sup>, reflections collected 12,547,  $R_{\text{int}} = 0.0364$ , data/parameters 4451/230, GOF on  $F^2$  1.021,  $R_I$  (all data) = 0.0550,  $wR_2$  (all data) = 0.1100.

The crystallographic data for Boc-Gly-(*E*)- $\Delta$ Phe-NHMe have been deposited at the Cambridge Crystallographic Data Centre as supplementary publication no CCDC 1814248. The data can be obtained free of charge via [www.ccdc.cam.ac.uk/conts/retrieving.html](http://www.ccdc.cam.ac.uk/conts/retrieving.html) (or from the Cambridge Crystallographic Data Centre, 12 Union Road, Cambridge CB2 1EZ, UK; fax: (+44) 1223 336,033; e-mail: deposit@ccdc.cam.ac.uk).

### Theoretical calculations

Gaussian 09 program package was used in all theoretical studies in this work [32].

### Geometry optimization

Starting geometries of the *E* and *Z* forms of the dipeptide Boc-Gly- $\Delta$ Phe-NHMe (see Fig. 1) were obtained from previously published conformers of Gly and  $\Delta$ Phe moieties [26]. The dihedral angles  $\phi$  and  $\psi$ , characteristic for minima of Ac-Gly-NHMe and Ac-(*E/Z*)- $\Delta$ Phe-NHMe, are collected in Table S1 (see the supplementary material). In addition, the standard  $\beta$ -turn conformations (characterized by main-chain torsion angles listed in Table S2 in the supplementary material) were also used as the starting structures in geometry optimization. We also took advantage of the achiral character of the studied molecules. Thus, only one conformer, defined by  $\phi_1, \psi_1, \phi_2, \psi_2$  dihedral angles were calculated. The other one with  $-\phi_1, -\psi_1, -\phi_2, \psi_2$ , being a mirror reflection was not considered since the conformational enantiomers have the same energy and spectral properties.

The initial structures were calculated using B3LYP/6-311++G(d,p) level of theory [33, 34]. As result, 28 local minima were

obtained (15 and 13 for **1** and **2**, respectively). The polarized continuum model PCM [35, 36] was used to include the effect of solvent. The presence of true minimum energy structures was confirmed by lack of imaginary harmonic frequencies. In addition, single point energy calculations were performed for all found conformers in the gas phase and solution using different level of theory, which better accounts dispersion interactions (MP2/6-311++G(d,p) and M06-2X/6-311++G(d,p) [37]).

**NMR calculations** Fully optimized B3LYP/6-311++G(d,p) structures of **1** and **2** in chloroform within the PCM model were applied as input for all nuclear magnetic shielding calculations using a standard gauge including atomic orbitals (GIAO) approach [38] and B3LYP functional. The calculated NMR parameters are sensitive to the electron correlation presence, method, and basis set. As result of previous tests, we decided to apply aug-cc-pVTZ-J basis set [39–41] in our NMR calculations. This basis set was downloaded from EMSL [42]. Obviously, it is a tailor-made basis set for spin-spin coupling constants in case of small molecules and as a good choice in the “locally dense basis set approach” [43, 44] for larger molecules. Fortunately, this “compact” basis set produces also good shieldings [45]. Chemical shifts were obtained using benzene and TMS as a reference. In addition, for efficient calculation of nuclear shieldings, we also used a newly modified STO-3G<sub>mag</sub> basis set [46]. Thus, we decided to test a performance of this basis set in case of NMR parameters of model peptides.

### IR spectra

The analytical grade  $CHCl_3$  was dried and distilled freshly before analysis. The infrared spectra were measured at room temperature (20 °C) with a Nicolet Nexus spectrometer flushed with dry  $N_2$ . The spectral resolution was set to 2 cm<sup>-1</sup>. Each spectrum was an average of 256 scans. The corresponding solvent spectra were used as a background removed during spectral processing. The solution of  $8.6 \cdot 10^{-3}$ – $1.7 \cdot 10^{-2}$  mol l<sup>-1</sup> concentration were measured in the 2.86 mm KBr liquid cell. All data processing was performed with the

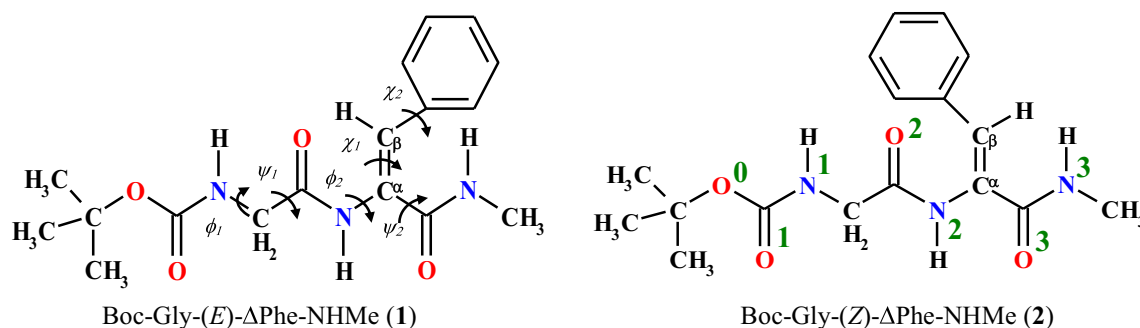


**Fig. 1** General formula, atom numbering and selected torsion angles for the studied compounds. Boc-Gly-(*E*)- $\Delta$ Phe-NHMe (**1**) Boc-Gly-(*Z*)- $\Delta$ Phe-NHMe (**2**).

GRAMS AI software [47]. The second derivatives and Fourier self-deconvolution techniques were applied to obtain the initial positions and numbers of bands in the N-H region of spectra. The accurate bands positions and intensities were estimated from mixed Gauss-Lorentz curve-fitting.

## NMR spectroscopy

Standard 1D  $^1\text{H}$  and  $^{13}\text{C}$  NMR spectra were recorded in  $\text{CDCl}_3$  with TMS as internal standard using Bruker Ultrashield 400 MHz NMR Spectrometer at room temperature. Data acquisition and processing were performed with standard Bruker TopSpin version 2.1 program. Unequivocal assignments of the  $^1\text{H}$  and  $^{13}\text{C}$  peaks for the studied peptides were accomplished according to a standard procedure [48] with the help of 2D homonuclear NOESY and ROESY experiments adjusting the values of mixing times and spinlock at 300 ms.

## Results and discussion

### X-ray crystal structure characterizes conformation and association pattern

The molecular structure of Boc-Gly-(*E*)- $\Delta$ Phe-NHMe (**1**) is depicted in Fig. 2. The majority of dimensions of the studied compound are, in principal, in agreement with related compounds [49–51]. There are, however, some differences, due to different intra- and intermolecular interactions. The torsion

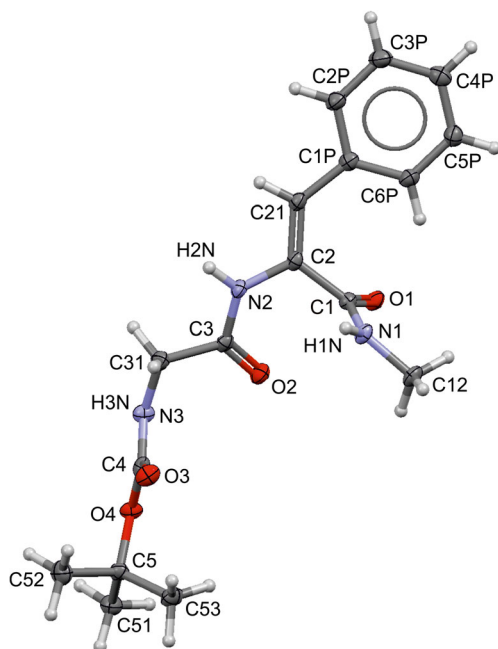


**Fig. 2** The molecular structure of Boc-Gly-(*E*)- $\Delta$ Phe-NHMe (**1**) in the crystalline state, showing the molecular conformation and the atom numbering scheme

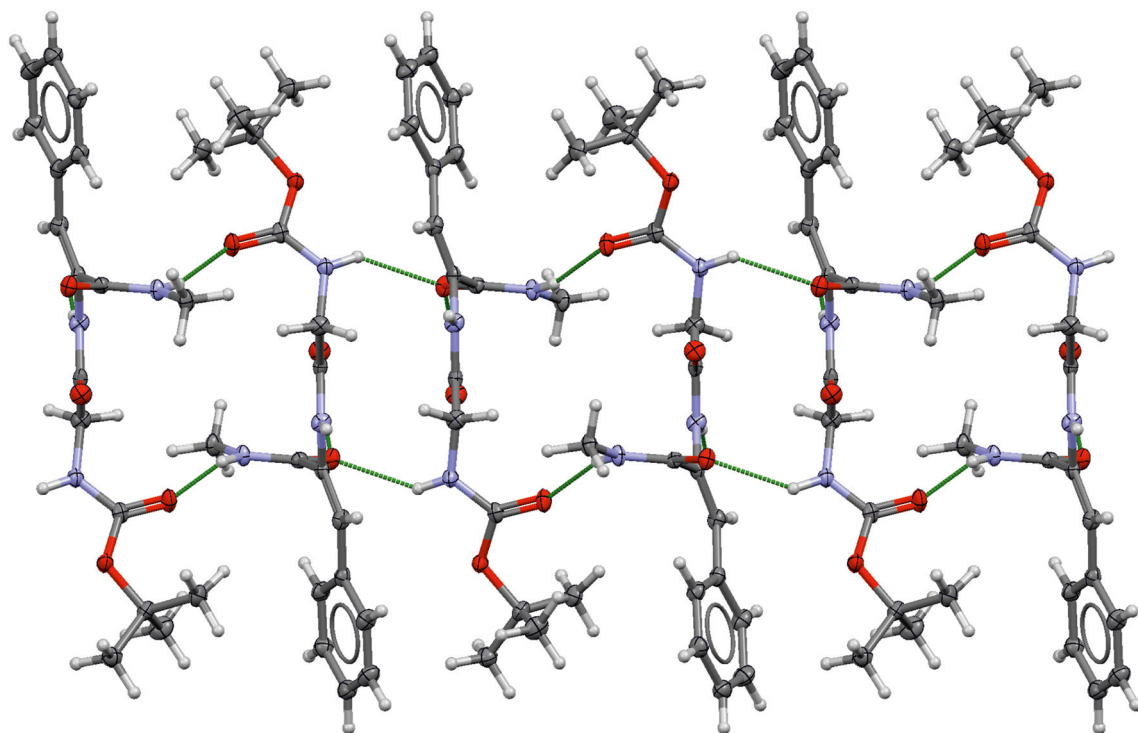
$\phi_1$ ,  $\psi_1$ ,  $\phi_2$ ,  $\psi_2$  angles for Boc-Gly-(*E*)- $\Delta$ Phe-NHMe are  $100.33(12)^\circ$ ,  $173.32(9)^\circ$  (Gly),  $-23.38(15)^\circ$  and  $-73.51(12)^\circ$  (*E*- $\Delta$ Phe). The opposite  $-\phi$  and  $-\psi$  angles were also found for the corresponding symmetry-related molecules. Apart from  $\phi_2$ , torsion C3-N2-C2-C21 ( $158.70(10)^\circ$ ), N2-C2-C21-C1P ( $173.53(11)^\circ$ ), and C2-C21-C1P-C2P ( $179.21(11)^\circ$ ) show that phenyl ring, C2 = C21 double bond, and N-terminal amide are basically coplanar indicating possible extended  $\pi$ -electron conjugation, whereas the C-terminal amide group is in perpendicular position resulting from a steric hindrance imposed by the phenyl ring at *E* position.

Figure 3 presents the association pattern of Boc-Gly-(*E*)- $\Delta$ Phe-NHMe in the crystal structure. Perpendicular position of the amide groups enables formation of the intermolecular N–H $\cdots$ O hydrogen bonds, which are responsible for the molecular association (Table S3). Each Boc-Gly-(*E*)- $\Delta$ Phe-NHMe molecule (serving as both hydrogen-bond donor and acceptor) is involved in six N–H $\cdots$ O hydrogen bonds, in which four are created by the (*E*)- $\Delta$ Phe flanking amide groups. The C-terminal amide group forms three N–H $\cdots$ O hydrogen bonds, involving C=O as bifurcated acceptor, whereas the N-terminal amide is involved as single N–H donor. As a result, the molecules bend in a way, which makes access to the N-terminal C=O group difficult. The weaker C–H $\cdots$ O intramolecular bonds play a supporting role and further stabilize the adopted molecular conformation (Table S3).

For *Z* analogue Boc-Gly-(*Z*)- $\Delta$ Phe-NHMe [52], the torsion  $\phi_1$ ,  $\psi_1$ ,  $\phi_2$ ,  $\psi_2$  angles are  $57.2(6)^\circ$ ,  $-141.2(4)^\circ$  (Gly),  $-71.5(6)^\circ$ , and  $-7.2(6)^\circ$  (*Z*- $\Delta$ Phe), respectively. The values of torsion  $\phi_2$ ,  $\psi_2$  indicate that C-terminal amide bond is coplanar with double bond and phenyl ring, and due to steric crowding imposed by the phenyl ring at the position *Z*, the N-terminal amide group is perpendicular to this molecular fragment. As a result, the perpendicular position of the N-terminal amide group enables formation of intermolecular N–H $\cdots$ O hydrogen bonds (Fig. 4). As can be seen, position of the phenyl ring in space, *Z* or *E*, changes the conformation of the  $\Delta$ Phe residue and influences the intermolecular pattern of hydrogen bonds interactions. It also has a profound effect on the torsion angles of neighboring Gly residue, and in consequence, on the whole molecular conformation.

### Theoretical calculations

$\alpha,\beta$ -Dehydrophenylalanine contains a  $\text{sp}^2$  hybridized carbon alpha resulting in conformations different from those shown by standard amino acids. In order to simplify the nomenclature and correctly characterize the non-typical conformation, we used the more versatile and convenient Zimmerman [53] notation. The *E*, *E*\*, *H* (or *F*), *C*, *D*, and *G*\* conformations correspond to the extended ( $\text{C}_5$ ),  $\alpha_{\text{D}}$ , polyproline-like ( $\beta$  or  $\text{P}_{\text{II}}$ ),  $\text{C}_7$ ,  $\beta_2$ , and  $\alpha'$  structures, reported in the literature. The direct comparison of the above-mentioned nomenclature



**Fig. 3** The association pattern of Boc-Gly-(*E*)- $\Delta$ Phe-NHMe (**1**) molecules in the crystal structure (only one single chain is shown for clarity). The green, dotted lines indicate the N-H $\cdots$ O hydrogen bonds

methods related to the characterization of backbone conformation and their position on the Ramachandran map is shown in Fig. S1 in the supplementary material. In the course of calculations, we decided to classify some geometries as  $\beta$ -turns by using the  $\tau$  and  $d$  parameters as selection criteria [54, 55]. The dihedral angle  $\tau$  ( $O^0-C^2-C^\alpha-C^4$ ) (Fig. 1) indicates the openness of a backbone chain, and  $d$  measures the separation between the  $O^0\cdots C^4$  atoms. The  $\tau$  and  $d$  parameters are gathered in Tables 1 and 3. For  $\beta$ -turn structures, marked

in bold in the tables, the following relations hold:  $|\tau| \leq 90^\circ$  and  $d \leq 7.0 \text{ \AA}$ .

#### Boc-Gly-(*E*)- $\Delta$ Phe-NHMe (**1**)

The selected parameters, including relative B3LYP/6-311++G(d,p) calculated energies of Boc-Gly-(*E*)- $\Delta$ Phe-NHMe in the gas phase and immersed in a polarizable continuum, whose dielectric constant matches that of chloroform or water, are gathered in Table 1. Only the conformers of (**1**) with relative energies lower than 1 kcal/mol in each environment are shown. An extended version of this table, showing all found conformers with relative energy less than 5 kcal/mol, is included in the supplementary material as Table S5. Additionally, both M06-2X and MP2 single point calculations, using the same basis set, were performed (see two last columns in Tables 1 and S5). According to the results of all used methods, in the gas phase the three most stable conformers of (**1**), with nearly identical energy are B\*E\*, EE\*, and B\*E. In all of them, the (*E*)- $\Delta$ Phe residue adopts an extended conformation. The remaining conformers have much higher relative energies. Also in the presence of chloroform and water, two or three lowest energy conformers have the (*E*)- $\Delta$ Phe residue in the extended conformation. Recently, we reported that the model Ac-(*E*)- $\Delta$ Phe-NHMe diamide [49], both in the gas phase and in solution, has a strong tendency to adopt extended conformation, although polar solvent significantly reduces energy difference between this

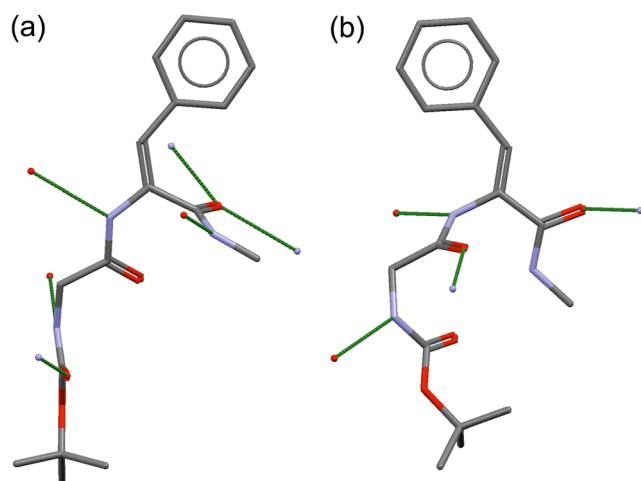


**Fig. 4** The different conformations adopted by Boc-Gly-(*E*)- $\Delta$ Phe-NHMe (**a**) and Boc-Gly-(*Z*)- $\Delta$ Phe-NHMe (**b**) isomers in their crystal structures. The dotted green lines represent intermolecular hydrogen bonds interactions (hydrogen atoms have been omitted for clarity)

**Table 1** The Boc-Gly-(E)- $\Delta$ Phe-NHMe conformers in the gas phase and in chloroform and water (within PCM model) characterized by dihedral angles and relative energies obtained by B3LYP, M06-2X, MP2/6-311++G(d,p) methods

Conformer code [ref. 53]	$\phi_1$ [°]	$\psi_1$ [°]	$\phi_2$ [°]	$\psi_2$ [°]	$\chi_2$ [°]	$\tau$ [°]	$d$ [Å]	$\Delta E$ [kcal/mol]		
								B3LYP	M06-2X	MP2
Gas phase								<b>B3LYP</b>	<b>M06-2X</b>	<b>MP2</b>
B*E*	114.5	-12.2	178.0	-155.1	52.5	-12.5	7.3	<b>0.00</b>	<b>0.00</b>	<b>0.00</b>
EE*	-177.1	-179.2	179.7	163.1	-58.7	-174.1	10.6	0.05	0.28	1.74
B*E	112.5	-9.3	-177.6	161.2	-57.3	17.8	7.3	0.18	0.15	0.15
chloroform								<b>B3LYP</b>	<b>M06-2X</b>	<b>MP2</b>
B*E*	111.3	-7.2	178.7	-148.0	47.2	-10.4	7.3	<b>0.00</b>	<b>0.00</b>	<b>0.00</b>
B*E	111.9	-5.2	-175.2	148.4	-45.8	28.8	7.4	0.22	0.20	0.13
E*E	177.3	-178.5	-179.2	153.7	-50.5	-163.7	10.6	0.87	1.08	2.58
water								<b>B3LYP</b>	<b>M06-2X</b>	<b>MP2</b>
B*E*	105.2	-1.2	179.3	-143.3	44.3	-6.0	7.2	<b>0.00</b>	<b>0.00</b>	0.10
B*E	106.1	0.0	-177.4	144.5	-44.2	32.7	7.3	0.02	0.04	0.16
B*C	107.3	-0.6	-40.8	127.1	-33.3	173.9	9.3	0.86	0.51	0.06
BC	-104.6	1.5	-41.2	127.4	-33.5	149.0	9.1	0.96	0.48	<b>0.00</b>
X-ray structure										
E*H	100.3	173.3	-23.4	-73.51	-1.9	-31.2	7.3	-	-	-

conformation and a second conformation H. Similarly, in larger system Ac-Gly-(E)- $\Delta$ Phe-NHMe, the (E)- $\Delta$ Phe residue in (E)- $\Delta$ Phe-NHMe fragment exists in an extended conformation in three of the lowest energy minima [26]. In the currently studied dipeptide **1**, we observe a similar conformational behavior of the (E)- $\Delta$ Phe residue.

Furthermore, the Gly residue adopts the B ( $\phi_1, \psi_1 \approx 113^\circ, -10^\circ$ ) conformation in the majority of found structures of dipeptide **1**. It is rather surprising because the results of the DFT and DFT-D3 calculations [56] indicate that the energy of this conformer for Ac-Gly-NHMe diamide model in the gas phase is rather high (its relative energy is about 2 kcal/mol). For this reason, we decided to check how the exchange of the Ac- by Boc- group affects the conformational preferences of Gly derivative.

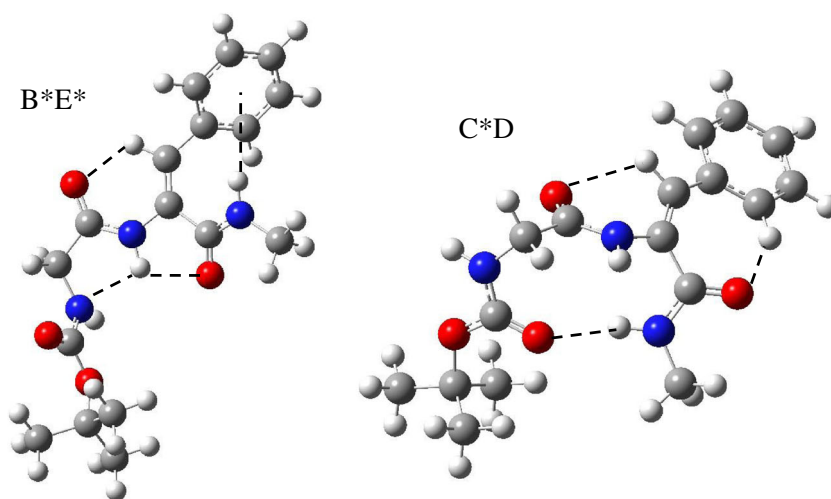
The results of B3LYP/6-311++G(d,p) calculations for Ac-Gly-NHMe (**3**) and Boc-Gly-NHMe (**4**) in the gas phase and in water are shown in Table 2.

As can be concluded from the results of the calculations presented in Table 2, exchange of Ac- group on Boc- has a negligible effect on the geometric parameters and the relative energies of E and C conformers. In contrast, there is a clear reduction of the relative energy of B conformer. The B structures of **3** and **4** are stabilized by N-H $\cdots$ N intramolecular hydrogen bonds and this interaction is stronger and shorter in the case of Boc-Gly-NHMe molecule. The N $\cdots$ H distances are 2.37 Å and 2.31 Å for **3** and **4**, respectively. For both of the studied molecules, **3** and **4** water most strongly stabilizes conformer B which in aqueous environment becomes a global

**Table 2** Selected conformational parameters and relative energies for Ac-Gly-NHMe (**3**) and Boc-Gly-NHMe (**4**) conformers in the gas phase and water calculated by B3LYP/6-311++G(d,p) method

Conformer	$\phi$ [°]	$\psi$ [°]	$\Delta E$ [kcal/mol]	
			Gas phase	Water
Ac-Gly-NHMe ( <b>3</b> )				
E (C <sub>5</sub> )	-179.9	179.9	0.42	180.0
C (C <sub>7</sub> )	82.5	-71.0	0.00	83.1
B	112.7	-17.1	2.03	99.9
F	-	-	-	-77.9
Boc-Gly-NHMe ( <b>4</b> )				
E (C <sub>5</sub> )	177.3	178.6	0.85	180.0
C (C <sub>7</sub> )	82.6	-69.0	0.00	83.7
B	117.9	-13.0	0.75	105.1
F	-	-	-	-77.0

**Fig. 5** The global minimum (B\*E\*) and the  $\beta$ -turn conformation (C\*D) for Boc-Gly-(*E*)- $\Delta$ Phe-NHMe (**1**) optimized at the B3LYP/6–311++G\*\* level of theory in the gas phase. The hydrogen bonds are marked by dashed lines



minimum. In the water environment for both molecules **3** and **4**, we found additional local minimum F, stabilized mainly by attractive interaction of the two carbonyl groups. This structure is similar to the conformation of the Gly residue in the Boc-Gly-(*E*)- $\Delta$ Phe-NHMe crystal ( $\phi, \psi = 100^\circ, 173^\circ$ ).

The presence of a number of subtle and simultaneous noncovalent interactions determines the conformation of a polypeptide chain. We assume in this study that both H-bond (N-H $\cdots$ O, N-H $\cdots$ N, N-H $\cdots$  $\pi$ , C-H $\cdots$ O) [57] and dipole-dipole forces [58] are the main factors, which determine the peptide conformation. On the other hand, we omit hyperconjugative effects [59, 60] in our considerations. The characteristic structural parameters for all intramolecular hydrogen bonds stabilizing conformers of the studied dipeptides are shown in Table S4 in the supplementary material.

It is important to notice that E conformation of (*E*)- $\Delta$ Phe residue is stable due to an extremely short N<sup>2</sup>-H $\cdots$ O<sup>3</sup> C<sub>5</sub> hydrogen bond (H $\cdots$ O<sup>3</sup> distance of 2.00 Å) and by C <sup>$\beta$</sup> -H $\cdots$ O<sup>2</sup> resonance assisted intramolecular H-bond (RAHB) [61]. This interaction leads to a formation of a six-member ring. In addition, the stabilization of this conformation causes the N<sup>3</sup>-H $\cdots$  $\pi$  hydrogen bonding with phenyl ring (Fig. 5).

According to B3LYP results in the gas phase, chloroform, and in water, the structure B\*E\* in Fig. 5 is the lowest energy conformer of **1**. This structure is stabilized by above-described interactions within the conformer E and B of (*E*)- $\Delta$ Phe and Gly residues, respectively. Second in energy order is the extended conformer EE\*, stabilized mainly by two N-H $\cdots$ O C<sub>5</sub> H-bonds. It is worth noting that increasing polarity of the environment causes a marked destabilization of this conformer. Moreover, the single point energies calculated with MP2 are much higher for this conformer in all studied environments (by about 1.7 kcal/mol and 1.5 kcal/mol in comparison to the B3LYP and M06-2X results, respectively).

Conformer C\*D of **1** is the lowest in energy  $\beta$ -turn structure and is characterized by a fairly high relative energy of 4.35 kcal/mol (Table S5 in the Supporting Information). This  $\beta$ -turn

conformer contains 1  $\leftarrow$  4 H-bond with the N<sup>3</sup>-H $\cdots$ O<sup>1</sup> distance equal to 2.11 Å. In addition, there are present two C-H $\cdots$ O interactions (see Fig. 5, as well as Table S4 in the Supporting Information). The torsion angle  $\chi_2$  is only  $-21^\circ$  and this suggests a partial  $\pi$ -electron conjugation of the phenyl ring of (*E*)- $\Delta$ Phe residue with the double bond C <sup>$\alpha$</sup> =C <sup>$\beta$</sup> . A comparison of backbone angles with the values for typical  $\beta$ -turns (see Table S2) indicates the C\*D conformation is a distorted Type II  $\beta$ -turn.

For the model diamide Ac-(*E*)- $\Delta$ Phe-NHMe, we observed a decrease of relative energy of helical conformer A\* as a result of increased solvent polarity [20]. A similar phenomenon was observed for a larger model derivative of (*E*)- $\Delta$ Phe [26, 49]. Also the investigation in this work molecule (**1**) shows an increased tendency to adopt a helical conformation with increasing polarity of the environment. Among the low energy conformers of (**1**) ( $\Delta E < 5$  kcal/mol) the (*E*)- $\Delta$ Phe residue adopts conformer A for 0, 2, and 4 structures in vacuo, chloroform, and water, respectively (see Table S5 in the Supporting Information).

### Boc-Gly-(*Z*)- $\Delta$ Phe-NHMe (**2**)

In the four lowest-energy structures ( $\Delta E \leq 1$  kcal/mol) of (**2**) in the gas phase (Table 3 and Table S6 in Supporting Information) obtained by B3LYP density functional the (*Z*)- $\Delta$ Phe residue adopts B conformation ( $\phi_2, \psi_2 \approx -60^\circ, 20^\circ$ ) which is stabilized by C<sub>7</sub> N<sup>3</sup>-H $\cdots$ O<sup>2</sup> H-bond. According to this method, the lowest energy structure of the **2** in vacuum is the conformer B\*B with the previously described conformation B\* on Gly residue stabilized by N<sup>2</sup>-H $\cdots$ N<sup>1</sup> hydrogen bond, and B conformation on the (*Z*)- $\Delta$ Phe residue (Fig. 6, Table S4). The BB conformer which is the second in energy order ( $\Delta E = 0.43$  kcal/mol), is stabilized by an almost identical system of hydrogen bonds as the B\*B conformer.

**Table 3** The Boc-Gly-(*Z*)- $\Delta$ Phe-NHMe conformers in the gas phase and in chloroform and water (within PCM model) characterized by dihedral angles and energy differences obtained by B3LYP, M06-2X, MP2/6-311++G(d,p) methods

Conformer code [Ref. 53]	$\phi_1$ [°]	$\psi_1$ [°]	$\phi_2$ [°]	$\psi_2$ [°]	$\chi_2$ [°]	$\tau$ [°]	<b>d</b> [Å]	$\Delta E$ [kcal/mol]		
								<b>B3LYP</b>	<b>M06-2X</b>	<b>MP2</b>
Gas phase								<b>B3LYP</b>	<b>M06-2X</b>	<b>MP2</b>
B*B	119.0	-11.1	-56.8	25.1	-27.5	139.9	8.60	<b>0.00</b>	1.04	0.46
BB	-114.8	9.5	-54.4	23.9	-39.0	133.7	8.43	0.43	2.02	1.67
<b>AB</b>	<b>-76.5</b>	<b>-13.3</b>	<b>-80.3</b>	<b>-3.6</b>	<b>-39.3</b>	<b>65.3</b>	<b>5.88</b>	0.88	<b>0.00</b>	<b>0.00</b>
EB	-171.0	177.5	-56.9	23.6	-35.2	-54.9	8.16	1.04	2.79	4.56
<b>CB*</b>	<b>-62.6</b>	<b>127.2</b>	<b>109.3</b>	<b>-11.8</b>	<b>-18.8</b>	<b>37.7</b>	<b>5.76</b>	1.11	0.84	0.48
in chloroform								<b>B3LYP</b>	<b>M06-2X</b>	<b>MP2</b>
<b>AA</b>	<b>-72.0</b>	<b>-19.5</b>	<b>-64.1</b>	<b>-15.2</b>	<b>-22.7</b>	<b>71.4</b>	<b>5.94</b>	<b>0.00</b>	<b>0.00</b>	<b>0.00</b>
BF*	-115.9	7.7	46.0	-141.2	28.6	-154.7	9.25	0.80	2.51	1.85
<b>CB*</b>	<b>-62.3</b>	<b>127.1</b>	<b>105.4</b>	<b>-12.3</b>	<b>-20.1</b>	<b>31.9</b>	<b>5.71</b>	1.23	1.51	1.55
B*B	119.6	-8.9	-60.2	26.9	-25.7	136.8	8.49	1.28	3.30	3.00
in water								<b>B3LYP</b>	<b>M06-2X</b>	<b>MP2</b>
<b>AA</b>	<b>-71.0</b>	<b>-20.9</b>	<b>-64.2</b>	<b>-16.2</b>	<b>-15.2</b>	<b>69.9</b>	<b>5.90</b>	<b>0.00</b>	<b>0.00</b>	<b>0.00</b>
BF*	-115.4	5.7	47.0	-142.9	28.0	-155.4	9.30	1.40	3.12	2.20
B*F*	106.9	-3.9	46.3	-142.4	27.6	-140.5	9.00	1.34	3.30	2.62
<b>FB*</b>	<b>-61.4</b>	<b>131.6</b>	<b>94.4</b>	<b>-8.4</b>	<b>-14.0</b>	<b>24.5</b>	<b>5.70</b>	1.73	2.06	2.68
X-ray structure [52]										
<b>FB*</b>	<b>-57.2</b>	<b>141.2</b>	<b>71.5</b>	<b>7.2</b>	<b>0.5</b>	<b>19.4</b>	<b>5.28</b>	–	–	–

We also found two conformations of **2**, which fulfill the  $\beta$ -turn criteria: AB and CB\*. The corresponding relative energies of these structures are 0.9 and 1.1 kcal/mol. Both conformations are stabilized by 1  $\leftarrow$  4 hydrogen bonds and their relative energy confirms repeatedly described in the literature tendency of (*Z*)- $\Delta$ Phe residue to stabilize  $\beta$ -turn conformation. It should be noted that the A conformation of the Gly residue was not found for the model molecules either **3** or **4**. It should rather be regarded as modified B conformation, because it is also stabilized by N<sup>2</sup>-H $\cdots$ N<sup>1</sup> hydrogen bond. Moreover, according to the results of MP2 and M06-2X methods conformer AB is the global minimum of **2**, and the

second  $\beta$ -turn structure (CB\*) has a much lower relative energy than is provided by B3LYP method. The latter structure is the global minimum of previously studied model dehydropeptide Ac-Gly-(*Z*)- $\Delta$ Phe-NHMe according the B3LYP and MP2 methods [26].

The results of B3LYP, M06-2X, and MP2 calculations indicate a significant stabilization of the  $\beta$ -turn structure of **2** by solvent. In chloroform and water environment, the global minimum is AA, which evolved from the AB conformation after small changes in  $\phi_2$ ,  $\psi_2$  torsion angles within the (*Z*)- $\Delta$ Phe residue. Both residues in this conformer exhibit a helical conformation, with  $\phi_2$ ,  $\psi_2$  angles of  $-64^\circ$  and  $-15^\circ$ . Similarly, the

**Fig. 6** The global minimum (B\*B) and the  $\beta$ -turn conformation (AB) for Boc-Gly-(*Z*)- $\Delta$ Phe-NHMe (**2**) obtained by B3LYP/6-311++G(d,p) method in the gas phase. The H-bonds are marked as dotted lines

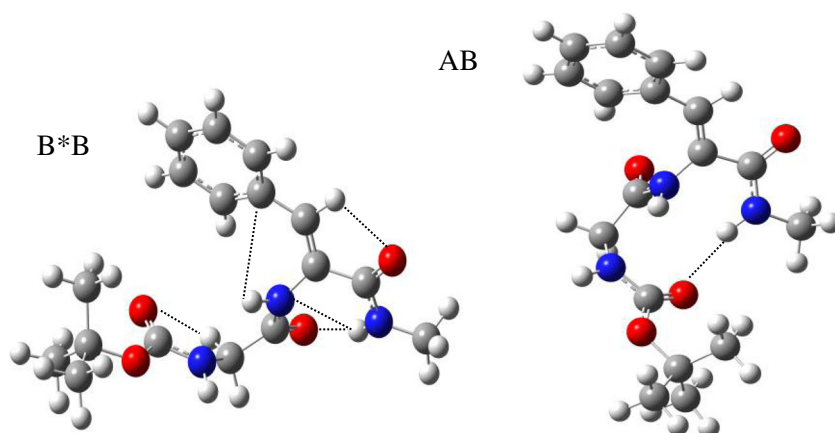
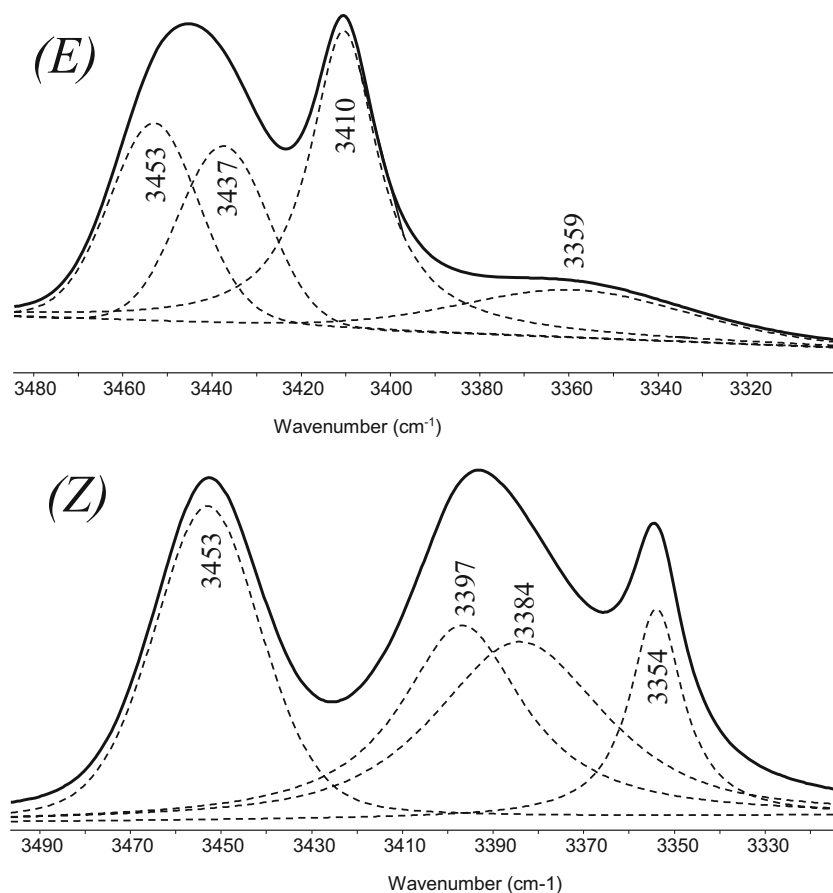




**Fig. 7** The  $\nu_s(\text{N-H})$  region of IR spectra of (*E*) and (*Z*) isomer of Boc-Gly- $\Delta$ Phe-NHMe in  $\text{CHCl}_3$  solution



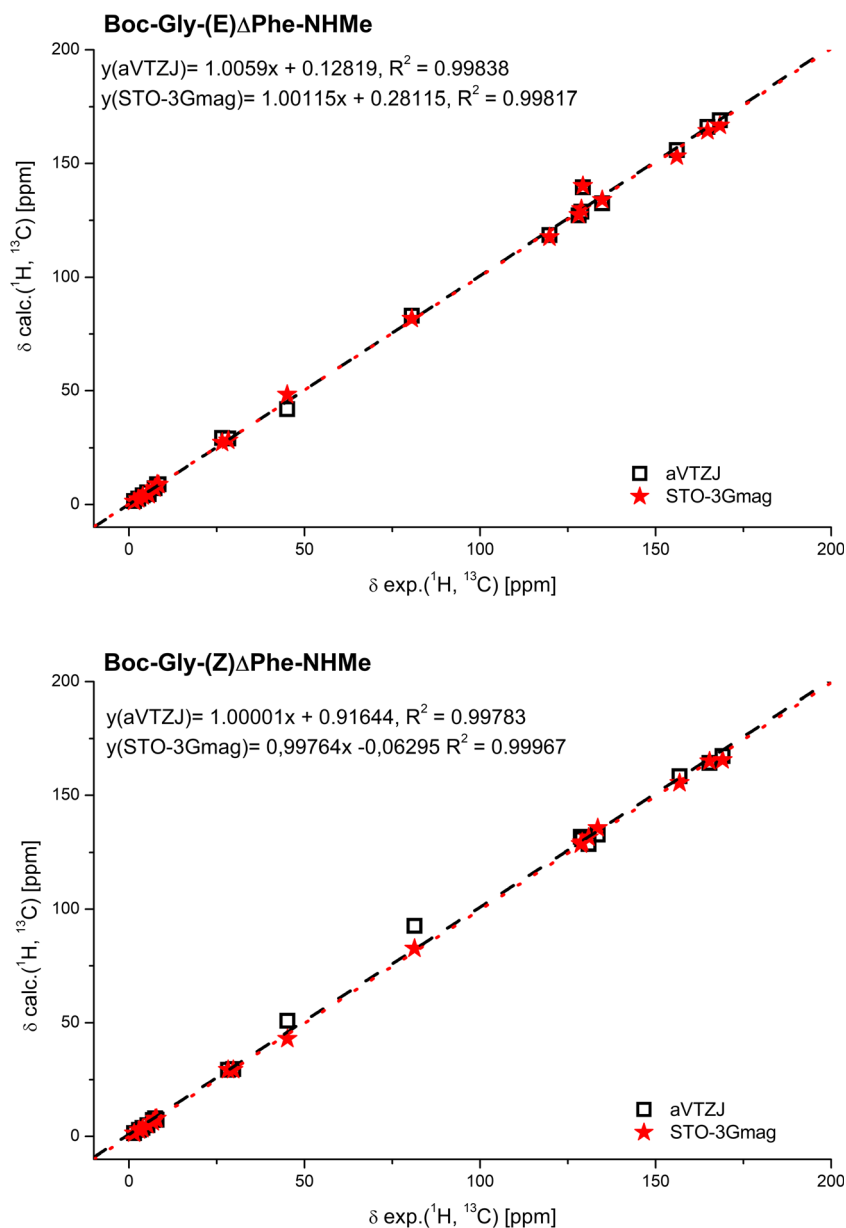
$3_{10}$ -type helix induced by solvent was recently observed for Ac-(*Z*)- $\Delta$ Phe-NHMe [49] and also in case of longer peptide

chain containing (*Z*)- $\Delta$ Phe residue [26]. Boc-Gly-(*Z*)- $\Delta$ Phe-NHMe exists in crystalline state as the  $\beta$ -turn Type II. This

**Table 4** B3LYP calculated and experimental  $^{13}\text{C}$  and  $^1\text{H}$  NMR chemical shifts for **E** and **Z** isomers of Boc-Gly- $\Delta$ Phe-NHMe in chloroform

Atom	Izomer <b>E</b>			Izomer <b>Z</b>		
	aug-ccpVTZ-J	STO-3G <sub>mag</sub>	Exp.	aug-ccpVTZ-J	STO-3G <sub>mag</sub>	Exp.
CH <sub>3</sub> [Boc]	29.30	27.22	26.55	29.34	29.28	28.24
CH <sub>3</sub> [NHMe]	29.12	28.26	28.28	29.59	29.30	29.71
C <sup>α</sup> [Gly]	42.00	48.26	45.09	50.88	43.01	45.16
C <sup>γ</sup> [Boc]	83.07	81.74	80.55	92.64	82.66	81.32
C <sup>α</sup> [ $\Delta^{E/Z}$ Phe]	132.51	134.03	134.79	131.66	128.54	128.76
C <sup>β</sup> [ $\Delta^{E/Z}$ Phe]	118.41	117.62	119.82	132.71	135.62	133.53
C <sup>γ</sup> [ $\Delta^{E/Z}$ Phe]	139.49	140.19	129.29	137.80	138.17	
C <sup>ε</sup> [ $\Delta^{E/Z}$ Phe]	127.15	127.39	128.12	130.57	129.29	129.08
C <sup>δ1,2</sup> , C <sup>ε1,2</sup> [ $\Delta^{E/Z}$ Phe]	128.72	129.94	128.87	128.62	131.52	130.91
C=O [Boc]	155.89	153.20	156.03	158.37	155.50	156.84
C=O [Gly]	169.02	166.76	168.28	167.32	165.62	169.07
C=O [ $\Delta^{E/Z}$ Phe]	166.16	164.37	164.76	164.32	165.07	165.32
CH <sub>3</sub> [Boc]	1.46	1.31	1.48	1.44	1.31	1.45
CH <sub>3</sub> [NHMe]	2.57	2.40	2.66	2.80	2.67	2.91
H <sup>α</sup> [Gly]	3.96	3.65	3.93	3.67	3.21	3.86
HN [Gly]	4.58	4.18	5.60	4.83	5.00	5.28
H <sup>β</sup> [ $\Delta^{E/Z}$ Phe]	8.88	8.86	8.02	7.91	7.66	7.49
H <sup>δ1,2</sup> , H <sup>ε1,2</sup> [ $\Delta^{E/Z}$ Phe]	7.20	7.13	7.34	7.51,	7.63,	7.58, 7.36
				7.20	7.10	
HN [ $\Delta^{E/Z}$ Phe]	8.91	8.70	8.42	7.14	6.34	6.81
HN [NHMe]	5.26	5.03	5.18	7.28	7.82	7.86
<b>RMS</b>	<b>1.74</b>	<b>1.73</b>		<b>2.18</b>	<b>1.68</b>	
cpu	33d 18 h 26 min	16 h 51 min		26d 6 h 17 min	17 h 52 min	

**Fig. 8** Calculated vs. experimental  $^1\text{H}$  and  $^{13}\text{C}$  chemical shifts for *E* and *Z* isomers of Boc-Gly- $\Delta$ Phe-NHMe in deuteriochloroform



conformation has the backbone angles ( $\phi_1, \psi_1, \phi_2, \psi_2 = -57^\circ, 141^\circ, 72^\circ, 7^\circ$ ) [52], analogues to those theoretically predicted for conformer FB\* in water.

From the relative energies, it was possible to determine the ratio of  $\beta$ -turn structures for **2** as 15, 62, and 79% in the gas phase, chloroform, and water, respectively. Such results indicate the high preference of dipeptide with (*Z*)- $\Delta$ Phe residue in the (*i* + 2) position to exist in polar media in bended form.

### FT-IR spectra

Three  $\nu_s(\text{N-H})$  bands, at 3445, 3410, and 3359  $\text{cm}^{-1}$ , are visible in the FT-IR spectrum of Boc-Gly-(*E*)- $\Delta$ Phe-NHMe (**1**) in  $\text{CHCl}_3$  solution (Fig. 7). On the basis of comparison between of Ac-(*E*)- $\Delta$ Phe-NHMe spectra in  $\text{CH}_2\text{Cl}_2$  solution

[21], we can assign the 3410 band to  $\nu_s(\text{N}^2\text{-H})$  vibration in  $\text{C}_5$  conformation of (*E*)- $\Delta$ Phe residue. The 3359  $\text{cm}^{-1}$  band is related to NH groups involved in intermolecular hydrogen bonds because the intensity of this band decreases with decreasing concentration of the peptide solution. The band at 3445 has a large half-width and is the result of a superposition of two bands: 3453 and 3437  $\text{cm}^{-1}$  due to  $\text{N}^1\text{-H}$  and  $\text{N}^3\text{-H}$  stretch modes, respectively. This assignment of band positions is consistent with the calculated IR spectrum of conformer B\*E\*. Thus, comparing IR spectrum of Boc-Gly-(*E*)- $\Delta$ Phe-NHMe (**1**) in  $\text{CHCl}_3$  solution with experimental spectra of similar molecular systems and with theoretical spectrum of B\*E\* conformer, one could assume that in chloroform solution peptide **1** exist in extended conformation within (*E*)- $\Delta$ Phe residue. In Fig. S3 in the Supplementary Material

are presented scaled theoretical infrared bands of N-H stretch modes superimposed on experimental spectra of (*E*) and (*Z*) isomers of Boc-Gly- $\Delta$ Phe-NHMe showing a reasonable agreement between predicted and observed spectra.

In the  $\nu_s(\text{N-H})$  region of the *Z* isomer spectrum three overlapping broad bands are observed. The accurate positions of four peaks were determined from a curve fitting: 3453, 3397, 3384, and 3354  $\text{cm}^{-1}$ . The 3354  $\text{cm}^{-1}$  band is concentration independent and, therefore, may be assigned to an intramolecularly hydrogen-bonded N-H group. Comparison with the calculated IR spectra for different Boc-Gly-(*Z*)- $\Delta$ Phe-NHMe conformers allows us to assign this band to  $\text{N}^3\text{-H}$  group in  $\beta$ -turn structures CB\* or AA. The 3453  $\text{cm}^{-1}$  originates from  $\text{N}^1\text{-H}$  group, and the bands 3397 and 3384  $\text{cm}^{-1}$  come from  $\text{N}^2\text{-H}$  group in two different  $\beta$ -turn conformation. This conclusion is consistent with the results of previous spectroscopic studies [62] on Boc-Ala-(*Z*)- $\Delta$ Phe-NHMe conformation in chloroform, where the authors also showed the occurrence of a significant population of type II  $\beta$ -turn structures with some evidence for the population of type I  $\beta$ -turn.

## $^1\text{H}$ and $^{13}\text{C}$ NMR spectra

Our earlier experiences [63] with prediction of proton and carbon NMR parameters in  $\text{CDCl}_3$  and  $\text{DMSO-d}_6$  solutions, calculated using B3LYP/aug-cc-pVTZ-J and PCM approach, pointed out the possibility of distinguishing between *E* and *Z* isomers of Ac- $\Delta$ Phe-NMe<sub>2</sub>.

In the current study, the experimental H-1 and C-13 chemical shifts of *E* and *Z* isomers of Boc-Gly- $\Delta$ Phe-NHMe in  $\text{CDCl}_3$  are accurately predicted (see Table 4). For *E* and *Z* isomers the calculated values are obtained for B\*E\* and AA conformers, respectively (they are the lowest energy structures in chloroform according to our calculations). Their presence in solution was also supported by IR data.

In case of  $\text{N}^2\text{H}$  signal, one can notice the biggest discrepancies between both isomers (shifted by about 1.6 ppm to lower magnetic field in *E* isomer) due to formation of intramolecular H-bond. Besides,  $\text{H}^b$  signal in *E* isomer is about 0.6 ppm shifted to the lower magnetic field. Very similar effects were observed in our earlier studies on *E* and *Z* isomers of Ac- $\Delta$ Phe-NMe<sub>2</sub>. [63]. Such large proton chemical shift differences could be explained by resonance-assisted H-bond in C<sub>5</sub> conformation of (*E*)- $\Delta$ Phe residue. In addition, a very large difference is observed for chemical shift of  $\text{N}^3\text{H}$  signal in *E* and *Z* isomers (5.18 and 7.49 ppm). This is due to formation of 1 ← 4 intramolecular H-bond by  $\text{N}^3\text{H}$  which stabilizes the  $\beta$ -turn structure. As expected, the chemical shift of *tert*-butyl group at about 1.5 ppm is very similar for both *Z* and *E* isomers.

In general, a nice theoretical reproduction of experimental positions of carbon signals is observed (Table 4). However, due to problems with solubility of the studied compounds in chloroform, the presence (and assignment) of  $\text{C}^\gamma$  [ $\Delta^{E/Z}$ Phe]

signal in the spectra is controversial (the difference between a theoretical chemical shift and a spectral feature buried in the noise is about 10 ppm).

The obtained results indicate a good performance of small STO-3G<sub>mag</sub> basis set with respect to a significantly larger aug-cc-pVTZ-J one (RMS of 2.74 vs. 2.76 ppm for isomer *E*, and 2.61 vs. 1.34 ppm for isomer *Z* in Table 4). The former basis set, being about half the size of the second one, yielded the magnetic shieldings significantly faster (CPU time of 17 h vs. 34 days, see Table 4).

The signal assignment of  $^1\text{H}$  and  $^{13}\text{C}$  spectra of the studied compounds was also supported by a linear correlation between theory and experiment (Fig. 8). The obtained linear equations indicate very similar performance of  $^1\text{H}$  and  $^{13}\text{C}$  chemical shifts of Boc-Gly-(*E*)- $\Delta$ Phe-NHMe isomer in  $\text{CDCl}_3$  ( $y = 1.006x + 0.128$ ,  $r^2 = 0.9984$  for aug-cc-pVTZ-J and  $y = 1.001x + 0.281$ ,  $r^2 = 0.9982$  for STO-3G<sub>mag</sub>). The correlations are similar for the *Z* isomer:  $y = 1.000x - 0.916$  ppm,  $r^2 = 0.9978$  and  $y = 0.9976x - 0.0630$ ,  $r^2 = 0.9997$ , for aug-cc-pVTZ-J and STO-3G<sub>mag</sub> basis respectively. In addition, we notice an overlap of points, calculated with both kinds of basis sets.

On the basis of the presented results, it is evident that molecular modeling is capable of selecting the dominant conformer in solution using the direct comparison between predicted and measured proton and carbon NMR signals [64].

## Conclusions

Among the promising ways of obtaining potentially active peptidomimetics is the inclusion of a dehydrophenylalanine residue into the peptide chain. Such structural modification leads to compounds with better proteolytic stability and increased hydrophobicity, resulting in improved blood-to-brain penetration, and rigidity of the molecular fragment.

Extensive theoretical calculations, as well as experimental X-ray, NMR, and IR methods were used to determine the conformational properties of *E* and *Z* isomers of Boc-Gly- $\Delta$ Phe-NHMe in chloroform. The presence of particular conformers of the studied isomers in solution, visible in IR and NMR spectra, was supported by theoretical calculations. Our studies revealed that the conformational preference of peptide backbone is strongly influenced by the position of the side chain in the  $\Delta$ Phe residue. The *E* isomer of dehydrophenylalanine shows a tendency to form an extended conformation both in vacuum and in polar media. However, increased polarity of the environment promotes the helical conformations of peptide with (*E*)- $\Delta$ Phe moiety.

The *Z* isomer of  $\Delta$ Phe promotes the formation of  $\beta$ -turn structure. According to our theoretical modeling and infrared spectra, the Boc-Gly-(*Z*)- $\Delta$ Phe-NHMe in chloroform solution exists as a mixture of  $\beta$ II and  $\beta$ III turns. Our results in solution are in good agreement with earlier X-ray studies. Methods

which account for dispersion (MP2 and M06-2X) work better than B3LYP in predicting the order of peptide conformers with respect to their relative energy. In this study, we also demonstrated a good agreement observed between chemical shifts calculated using small STO-3G<sub>mag</sub> basis sets and the dedicated ones.

**Acknowledgments** All the calculations were performed in WCSS Wrocław (<http://www.wcss.wroc.pl>) and in CYFRONET, AGH, Kraków, within a MEiN/SGI3700/UOpolski/063/2006 grant.

## Compliance with ethical standards

**Conflict of interest** The authors declare that they have no conflict of interest.

**Open Access** This article is distributed under the terms of the Creative Commons Attribution 4.0 International License (<http://creativecommons.org/licenses/by/4.0/>), which permits unrestricted use, distribution, and reproduction in any medium, provided you give appropriate credit to the original author(s) and the source, provide a link to the Creative Commons license, and indicate if changes were made.

## References

- Bock JE, Gavenonis J, Kritzer JA (2013) Getting in shape: controlling peptide bioactivity and bioavailability using conformational constraints. *ACS Chem Biol* 8:488–499
- Crisma M, De Zotti M, Fornaggio F, Peggion C, Moretto A, Toniolo C (2015) Handedness preference and switching of peptide helices. Part II: helices based on noncoded  $\alpha$ -amino acids. *J Pept Sci* 21:148–177
- Asfaw H, Laqua K, Walkowska AM, Cunningham F, Martinez-Martinez MS, Cuevas-Zurita JC, Ballell-Pages L, Imming P (2017) Design, synthesis and structure-activity relationship study of wollamide B; a new potential anti TB agent. *PLoS One* 12: e0176088
- Graue A, König B (2009) Peptidomimetics - a versatile route to biologically active compounds. *Eur J Org Chem* 30:5099–5111
- Hruby VJ (1982) Conformational restrictions of biologically active peptides via amino acid side chain groups. *Life Sci* 31:189–199
- Mathur P, Ramakumar S, Chauhan VS (2004) Peptide design using  $\alpha, \beta$ -dehydro amino acids: from  $\beta$ -turns to helical hairpins. *Biopolymers* 76:150–161
- Siodlak D (2015)  $\alpha, \beta$ -Dehydroamino acids in naturally occurring peptides. *Amino Acids* 47:1–17
- Jiang J, Ma Z, Castle SL (2015) Bulky  $\alpha, \beta$ -dehydroamino acids: their occurrence in nature, synthesis, and applications. *Tetrahedron* 71:5431–5451
- Mosberg HI, Dua RK, Pogozheva ID, Lomize AL (1996) Development of a model for the  $\delta$ -opioid receptor pharmacophore. 4. Residue 3 dehydrophenylalanine analogues of Tyr-C[D-Cys-PheD-Pen]OH (JOM-13) confirm required gauche orientation of aromatic side chain. *Biopolymers* 39:287–296
- Videira RA, Andrade PB, Monteiro LS, Valentão P, Ferreira PMT, Pereira DM (2018) Toxicity and structure-activity relationship (SAR) of  $\alpha, \beta$ -dehydroamino acids against human cancer cell lines. *Toxicol in Vitro* 47:26–37
- Vilaça H, Pereira G, Castro TG, Hermenegildo BF, Shi J, Faria TQ, Micaêlo N, Brito RMM, Xu B, Castanheira EMS, Martins JA, Ferreira PMT (2015) New self-assembled supramolecular hydrogels based on dehydropeptides. *J Mater Chem B* 3:6355–6367
- Adessi C, Soto C (2002) Converting a peptide into a drug: strategies to improve stability and bioavailability. *Curr Med Chem* 9:963–978
- Gupta M, Chauhan VS (2011) De novo design of  $\alpha, \beta$ -didehydrophenylalanine containing peptides: from models to applications. *Biopolymers* 95:161–173
- Gupta M, Acharya R, Mishra A, Ramakumar S, Ahmed F, Chauhan VS (2008) Dehydrophenylalanine ( $\Delta$ Phe) as a  $\beta$  breaker: extended structure terminated by a  $\Delta$ Phe-induced turn in the pentapeptide Boc-Phe1-Ala2-Ile3- $\Delta$ Phe4-Ala5-OMe. *Chem Bio Chem* 9: 1375–1378
- Jewginski M, Latajka R, Krezel A, Haremza K, Makowski M, Kafarski P (2013) Influence of solvents on conformation of dehydropeptides. *J Mol Struct* 1035:129–139
- Lisowski M, Jaremko Ł, Jaremko M, Mazur A, Latajka R, Makowski M (2010) Effect of the  $\Delta$ Phe residue configuration on a didehydropeptides conformation: a combined CD and NMR study. *Biopolymers* 93:1055–1064
- Makowski M, Lisowski M, Mikołajczyk I, Lis T (2007) N-[tert-Butoxycarbonylglycyl-(E)- $\alpha, \beta$ -dehydrophenylalanyl]glycylglycyl-(E)- $\alpha, \beta$ -dehydrophenylalanyl]glycine. *Acta Cryst Sect E* 63:19–21
- Makowski M, Lisowski M, Maciąg A, Lis T (2006) N-[tert-Butoxycarbonylglycyl-(Z)- $\alpha, \beta$ -dehydrophenylalanyl]glycyl-(E)- $\alpha, \beta$ -dehydrophenylalanyl] glycine methyl ester dihydrate. *Acta Cryst Sect E* 62:807–810
- Makowski M, Brzuszkiewicz A, Lisowski M, Lis T (2005) N-[tert-butoxycarbonylglycyl-(Z)- $\alpha, \beta$ -dehydrophenylalanyl]glycyl-(E)- $\alpha, \beta$ -dehydrophenylalanyl]phenylalanyl]-4-nitroaniline ethanol solvate. *Acta Cryst Sect C* 61:424–426
- Buczek A, Siodlak D, Bujak M, Broda MA (2011) Effects of side-chain orientation on the backbone conformation of the dehydrophenylalanine residue. Theoretical and X-ray study. *J Phys Chem B* 115:4295–4306
- Broda MA, Siodlak D, Rzeszotarska B (2005) Conformational investigation of  $\alpha, \beta$ -dehydropeptides. N-acetyl-(E)-dehydrophenylalanine N'-methylamide: conformational properties from infrared and theoretical studies, part XIV. *J Pept Sci* 11:235–244
- Latajka R, Makowski M, Jewginski M, Pawelczak M, Koroniak H, Kafarski P (2006) Peptide p-nitrophenylanilides containing (E)-dehydrophenylalanine - synthesis, structural studies and evaluation of their activity towards cathepsin C. *New J Chem* 30:1009–1018
- Latajka R, Jewginski M, Makowski M, Pawelczak M, Huber T, Sewald N, Kafarski P (2008) Pentapeptides containing two dehydrophenylalanine residues - synthesis, structural studies and evaluation of their activity towards cathepsin C. *J Pept Sci* 14: 1084–1095
- Latajka R, Jewginski M, Makowski M, Krezel A, Paluch S (2008) Conformational studies of hexapeptides containing two dehydroamino acid residues in positions 2 and 5 in peptide chain. *Biopolymers* 89:691–699
- Broda MA, Ciszak MA, Kozioł AE, Pietrzyński G, Rzeszotarska B (2006) Conformational investigation of  $\alpha, \beta$ -dehydropeptides. XVI.  $\beta$ -turn tendency in Ac-Pro- $\Delta$ Xaa-NHMe: crystallographic and theoretical studies. *J Pept Sci* 12:538–549
- Buczek A, Wałęsa R, Broda MA (2012)  $\beta$ -turn tendency in N-methylated peptides with dehydrophenylalanine residue: DFT study. *Biopolymers* 97:518–528
- Makowski M, Rzeszotarska B, Kubica Z, Wiczorek P (1984) Synthesis of peptides with  $\alpha, \beta$ -Dehydroamino acids, I. synthesis of N-benzyloxycarbonyl and N-trifluoroacetyl dipeptides of dehydroalanine and dehydrophenylalanine. *Liebigs Ann Chem* 5: 920–928
- Makowski M, Rzeszotarska B, Kubica Z, Pietrzyński G (1985) Synthesis of peptides with  $\alpha, \beta$ -dehydroamino acids, II. Synthesis

- of tert-butyloxycarbonyldipeptides of dehydroalanine and dehydrophenylalanine. *Liebigs Ann Chem* 5:893–900
29. CrysAlis CCD (ver. 171.33.57) and CrysAlis Pro (ver. 171.33.61), Oxford Diffraction Ltd., 2010
  30. Sheldrick GM (2008) A short history of SHELX. *Acta Crystallogr Sect A* 64:112–122
  31. Macrae CF, Bruno IJ, Chisholm JA, Edgington PR, McCabe P, Pidcock E, Rodriguez-Monge L, Taylor R, van de Streek J, Wood PA (2008) Mercury CSD 2.0 - new features for the visualization and investigation of crystal structures. *J Appl Crystallogr* 41:466–470
  32. Frisch MJ, Trucks GW, Schlegel HB, Scuseria GE, Robb MA, Cheeseman JR, Scalmani G, Barone V, Mennucci B, Petersson GA, Nakatsuji H, Caricato M, Li X, Hratchian HP, Izmaylov AF, Bloino J, Zheng G, Sonnenberg JL, Hada M, Ehara M, Toyota K, Fukuda R, Hasegawa J, Ishida M, Nakajima T, Honda Y, Kitao O, Nakai H, Vreven T, Montgomery Jr JA, Peralta JE, Ogliaro F, Bearpark M, Heyd JJ, Brothers E, Kudin KN, Staroverov VN, Kobayashi R, Normand J, Raghavachari K, Rendell A, Burant JC, Iyengar SS, Tomasi J, Cossi M, Rega N, Millam NJ, Klene M, Knox JE, Cross JB, Bakken V, Adamo C, Jaramillo J, Gomperts R, Stratmann RE, Yazyev O, Austin AJ, Cammi R, Pomelli C, Ochterski JW, Martin RL, Morokuma K, Zakrzewski VG, Voth GA, Salvador P, Dannenberg JJ, Dapprich S, Daniels AD, Farkas O, Foresman JB, Ortiz JV, Cioslowski J, Fox DJ (2009) Gaussian 09, Revision B.01. Gaussian, Inc., Wallingford
  33. Becke AD (1988) Density-functional exchange-energy approximation with correct asymptotic behavior. *Phys Rev A* 38:3098–3100
  34. Lee C, Yang W, Parr RG (1988) Development of the Colle-Salvetti correlation-energy formula into a functional of the electron density. *Phys Rev B* 37:785–789
  35. Miertuš S, Scrocco E, Tomasi J (1981) Electrostatic interaction of a solute with a continuum. A direct utilization of AB initio molecular potentials for the prevision of solvent effects. *Chem Phys* 55:117–129
  36. Tomasi J, Mennucci B, Cammi R (2005) Quantum mechanical continuum solvation models. *Chem Rev* 105:2999–3093
  37. Zhao Y, Truhlar DG (2008) The M06 suite of density functionals for main group thermochemistry, thermochemical kinetics, noncovalent interactions, excited states, and transition elements: two new functionals and systematic testing of four M06-class functionals and 12 other functionals. *Theor Chem Accounts* 120:215–241
  38. Wolinski K, Hinton JF, Pulay PJ (1990) Efficient implementation of the gauge-independent atomic orbital method for NMR chemical shift calculations. *J Am Chem Soc* 112:8251–8260
  39. Enevoldsen T, Oddershede J, Sauer SPA (1998) Correlated calculations of indirect nuclear spin-spin coupling constants using second-order polarization propagator approximations: SOPPA and SOPPA (CCSD). *Theor Chem Accounts* 100:275–284
  40. Provasi PF, Aucar GA, Sauer SPA (2001) The effect of lone pairs and electronegativity on the indirect nuclear spin-spin coupling constants in CH<sub>2</sub>X (X=CH<sub>2</sub>, NH, O, S): Ab initio calculations using optimized contracted basis sets. *J Chem Phys* 115:1324–1334
  41. Krivdin LB, Sauer SPA, Peralta JE, Contreras RH (2002) Non-empirical calculations of NMR indirect carbon-carbon coupling constants: 1. Three-membered rings. *Magn Reson Chem* 40:187–194
  42. EMSL basis set exchange. <https://bse.pnl.gov/bse/portal>
  43. Chesnut DB, Moore KD (1989) Locally dense basis sets for chemical shift calculations. *J Comput Chem* 10:648–659
  44. Chesnut DB, Byrd EFC (1996) The use of locally dense basis sets in correlated NMR chemical shielding calculations. *Chem Phys* 213:153–158
  45. Kupka T, Stachów M, Nieradka M, Kaminsky J, Pluta T (2010) Convergence of nuclear magnetic shieldings in the Kohn-Sham limit for several small molecules. *J Chem Theor Comput* 6:1580–1589
  46. Voronkov E, Rossikhin V, Okovyty S, Shatckih A, Bolshakov V, Leszczynski J (2012) Novel physically adapted STO ##-3G basis sets. Efficiency for prediction of second-order electric and magnetic properties of aromatic hydrocarbons. *Int J Quant Chem* 112:2444–2449
  47. GRAMS/AI Version 9.00 R2, Thermo Fisher Scientific Inc. 2009
  48. Goddard TD, Kneller DG. SPARKY 3; University of California: San Francisco, 2003
  49. Buczek A, Makowski M, Jewginski M, Latajka R, Kupka T, Broda MA (2014) Toward engineering efficient peptidomimetics. Screening conformational landscape of two modified dehydroaminoacids. *Biopolymers* 101:28–40
  50. Siodlak D, Broda MA, Rzeszotarska B, Dybała I, Koziol AE (2003) Conformational investigation of  $\alpha,\beta$ -dehydropeptides. XI. Molecular and crystal structure of Ac-(Z)- $\Delta$ Phe-NMe<sub>2</sub> as compared to those of related molecules. *J Pept Sci* 9:64–74
  51. Souhassou M, Lecomte C, Ghermani N-E, Rohmer MM, Wiest R, Benard M, Blessing RH (1992) Electron distributions in peptides and related molecules. 2. An experimental and theoretical study of (Z)-N-acetyl- $\alpha,\beta$ -dehydrophenylalanine methylamide. *J Am Chem Soc* 114:2371–2382
  52. Singh TP, Narula P, Chauhan VS, Kaur P (1989) Crystal structure and molecular conformation of the peptide N-Boc-L-glycyl-dehydro-Phe-NHCH<sub>3</sub>. *Biopolymers* 28:1287–1294
  53. Zimmerman SS, Pottle MS, Némethy G, Scheraga HA (1977) Conformational analysis of the 20 naturally occurring amino acid residues using ECEPP. *Macromolecules* 10:1–9
  54. Perczel A, McAllister MA, Csaszar P, Csizmadia IG (1993) Peptide models 6. New  $\beta$ -turn conformations from ab initio calculations confirmed by x-ray data of proteins. *J Am Chem Soc* 115:4849–4858
  55. Perczel A, Jakli I, McAllister MA, Csizmadia IG (2003) Intrinsically stable secondary structure elements of proteins: a comprehensive study of folding units of proteins by computation and by analysis of data determined by X-ray crystallography. *Chem Eur J* 9:2551–2566
  56. Cormanich RA, Rittner R, Bühl M (2015) Conformational preferences of Ac-Gly-NHMe in solution. *RSC Adv* 5:13052–13060
  57. Steiner T (2002) The hydrogen bond in the solid state. *Angew Chem Int Ed* 41:48–76
  58. Allen FH, Baalham CA, Lommerse JPM, Raithby PR (1998) Carbonyl-carbonyl interactions can be competitive with hydrogen bonds. *Acta Cryst Sect B* 54:320–329
  59. Cormanich RA, Ducati LC, Tormena CF, Rittner R (2013) A theoretical investigation of the dictating forces in small amino acid conformational preferences: the case of glycine, sarcosine and N, N-dimethylglycine. *Chem Phys* 421:32–38
  60. Cormanich RA, Bühl M, Rittner R (2015) Understanding the conformational behaviour of Ac-Ala-NHMe in different media. A joint NMR and DFT study. *Org Bio Chem* 13:9206–9213
  61. Crisma M, Formaggio F, Toniolo C, Yoshikawa T, Wakamiya T (1999) Flat peptides. *J Am Chem Soc* 121:3272–3278
  62. Kaur P, Uma K, Balam P, Chauhan VS (1989) Synthetic and conformational studies on dehydrophenylalanine containing model peptides. *Int J Peptide Protein Res* 33:103–109
  63. Buczek A, Ptak T, Kupka T, Broda MA (2011) Experimental and theoretical NMR and IR studies of the side-chain orientation effects on the backbone conformation of dehydrophenylalanine residue. *Magn Reson Chem* 49:343–349
  64. Nazarski RB, Wałejko P, Witkowski S (2016) Multi-conformer molecules in solutions: an NMR-based DFT/MP2 conformational study of two glucopyranosides of a vitamin e model compound. *Org Biomol Chem* 14:3142–3158